Proceedings of the 2024 Winter Simulation Conference
H. Lam, E. Azar, D. Batur, S. Gao, W. Xie, S. R. Hunter, and M. D. Rossetti, eds.

A MENTORED EXPERIENCE ACCUMULATION DIFFERENTIAL MODEL: RAPID PARAMETER SPACE ANALYSIS APPLIED TO ROYAL CANADIAN AIR FORCE PILOT PRODUCTION, ABSORPTION AND RETENTION

Jack Quirion, Stephen Okazawa, Robert Mark Bryce, and Jillian Anne Henderson

Centre for Operational Research and Analysis, Defence Research and Development Canada, Department of National Defence, Ottawa, ON, CANADA

ABSTRACT

Since the early 2000s, the Royal Canadian Air Force (RCAF) has used a detailed personnel training model—Pilot Production, Absorption, Retention Simulation (PARSim)—to study the progress of pilots from recruitment to release. The model captures key dynamics of pilot career throughput, with particular attention paid to the upgrade of inexperienced pilots arriving at operational squadrons via mentoring by experienced pilots. Here we develop a simplified model of the same career structure, based on systems of differential equations, that captures the fundamental dynamics and constraints of the full PARSim model but enables rapid analysis of the parameter space via numerical simulation to produce a higher level view of pilot occupation health. A further advantage of this model is that, within certain domains, the equations can be solved analytically which provides valuable insights into the system's stability, steady state, and critical conditions in terms of the model's fundamental parameters.

1 INTRODUCTION

Training pilots in the Royal Canadian Air Force (RCAF) is complex and resource intensive, with the cost of training a fighter pilot having been estimated to be between five and ten million dollars for modern platforms (Mattock et al. 2019). Combined with air assets being crucial for deterrence, intelligence and reconnaissance, defense, and offense—and air officers being used to staff senior roles in the Canadian Armed Forces (CAF)—managing the pilot occupation to ensure sufficient production, absorption (into a squadron), and retention is both a high priority and a significant challenge. Explored here are the resulting dynamics of this occupation structure (Section 2). Additional factors that affect retention include a strong draw from industry, high stress, and remote base locations that can negatively affect families and work-life balance, all of which can result in elevated attrition, an aspect that we can empirically measure and use in our models (Bryce and Henderson 2023).

Historically, the Centre for Operational Research and Analysis (CORA) in Defence Research and Development Canada (DRDC) has provided analytic support to decision makers in the context of the pilot community using the Pilot Production, Absorption, Retention Simulation (PARSim) model. This detailed model captures the flow of pilots from recruitment, through initial flight training, to their operational training unit, through their operational flying careers as mentees and subsequently as mentors, to senior staff positions, and ultimately to release from the CAF. It was first developed in the early 2000s in response to Chief of the Air Staff direction regarding pilot regeneration (Corbett 2013). PARSim has been used extensively in the decades since to study and plan for RCAF pilot community sustainability in the face of policy, market forces, and other changes that affect the occupation (Séguin 2015).

An advantage of detailed simulation models, like PARSim, is that complex behavior can be captured and specific what-if scenarios explored to determine their likely outcome, whether desirable or not. However, the associated disadvantage of such models is that it is usually infeasible, in terms of effort and computational cost, to explore the full parameter space to find regions that have either positive (i.e., stable and healthy) or

979-8-3315-3420-2/24/$31.00 ©2024 European Union

negative (i.e., unstable or infeasible) outcomes. To date PARSim has been used as a detailed what-if analysis tool solely by CORA analysts due to the complexity of the model and software implementation—originally a system dynamics model (Corbett 2013) which has recently been reimplemented as a Discrete Event Simulation (DES) model in Python using the Operational Research Integrated Graphical Analysis and Modelling Environment (ORIGAME) (Okazawa 2013; ORIGAME GitHub repository 2024). It was thus desirable to develop a simplified model with a reduced parameter set that could run faster and produce results across a wide parameter space. This would enable the broader analysis of what conditions constitute a healthy pilot population, and a simpler and less-costly assessment of whether a particular situation appears to be sustainable or not. Specific scenarios that are on the borderline of health in this simpler model can then be explored in greater detail in the full PARSim model.

Here we develop this simplified model of the pilot population, representing the core flows and constraints affecting the system using systems of differential equations. We focus on the experienced mentor population, as they are required to absorb new pilots (mentees) and supply senior staff positions and are thus a critical limiting component that directly relates to the health of the occupation. We call this model the Mentored Experience Accumulation Differential (MEAD) model to emphasize the key relationships being captured.

The use of models based on differential equations to describe military populations is a well-established approach, with early work using Markov models going back to the second world war (Seal 1945), and (Bartholomew et al. 1991) being a classic text outlining Markov and related models. This class of models represent standard continuous approaches to modelling population dynamics (Vincent and Okazawa 2019), whereas DES models typically treat populations as sets of discrete entities and population movements as stochastic events (Henderson 2019). Ideally, the relationship between discrete stochastic processes and continuous differential models is that the continuous model captures the expectation, or average, of the stochastic outcome of discrete models (see, for example, (Bryce and Henderson 2023)). The CAF uses a number of both Markov and DES based models for workforce analysis (Boileau 2012). However, most of these models do not incorporate mentee-mentor dynamics with experience accumulation, but rather implement push or pull movements between groups (see (Vincent and Okazawa 2019) for a clear discussion of push and pull promotions). There is a body of work that considers mentee-mentor dynamics by casting it into the predator-prey model and explores the stability and controllability of such systems, see, for example, (Schaffel et al. 2021) and (Lahteenmaa-Swerdlyk and Bourque 2024). In our work, we model a more complex mentee-mentor dynamic that includes important additional constraints relevant to flight training, specifically, a cap on flying positions and limited flying resources, constraints that are present in the full PARSim model (Séguin 2015). Although we can rapidly simulate a given scenario by solving the equations numerically, we also show that, within specified domains, the equations can be solved analytically. These analytical solutions provide important insights into the stability, steady state conditions and critical states of the system; insights that cannot be derived from more complex implementations of the PARSim model.

Because of MEAD's relative simplicity, allowing scenarios to be rapidly characterized and simulated, we also created a web tool, which is accessible to analysts, military staff, and decision makers alike. This tool consists of an easy to use web interface where users input parameters describing the pilot occupation (Section 2) and generate plots that visualize the system across various parameter spaces (Section 3).

2 THE MENTORED EXPERIENCE ACCUMULATION DIFFERENTIAL (MEAD) MODEL

The components of the PARSim model for a single fleet's pilot population are depicted in the flow diagram of Figure 1. The career model flow is divided into four regions consisting of initial pilot training activities (lower left) leading to the operational squadron as an inexperienced (mentee) pilot, I, (upper left) transitioning to an experienced (mentor) pilot, E, (upper right), then moving to and from non-operational staff positions, N, (lower right). Losses from the mentor portion of the population are accounted for via an attrition rate parameter, α, and other losses, h, that include postings to senior staff positions (upper right). Due to the restricted release of new pilots in the RCAF, losses from the mentee portion of the population are considered negligible and are not modelled. Upgrading is the process by which mentees transition to

mentors, and the rate at which this occurs is the central aspect of the model. In reality, pilot upgrading is a more complex, multi-levelled process with many internal and external dependencies, but military planners are primarily concerned with a simplified division into inexperienced (mentee) and experienced (mentor) pilots and seek the control the ratio between the two. Both PARSim and MEAD include this simplified upgrade process, where a single transitional rate, u, captures the rate at which inexperienced pilots gain experience and upgrade via mentoring from experienced pilots. The upgrade rate depends on the number of inexperienced and experienced pilots, and "flying hours"—a parameter that encapsulates the maximum annual aircraft availability and budget allocation with the cap set by decision makers, referred to as the Yearly Flying Rate (YFR). We refer the reader to (Corbett 2013) for a thorough description of the full PARSim model and to (Séguin 2015) which presents a real case study.

The pared-down elements of this model captured in MEAD are shown in bold in Figure 1, which remove the details of the initial pilot training (replaced by a single intake rate parameter, g), advanced training (which has minimal impact on overall pilot numbers), and the re-training of non-operational pilots (where the staffing flow, s, is a net bi-directional flow). In addition to the level of detail, for an equivalent scenario a key difference between the models is MEAD is continuous while PARSim is discrete.

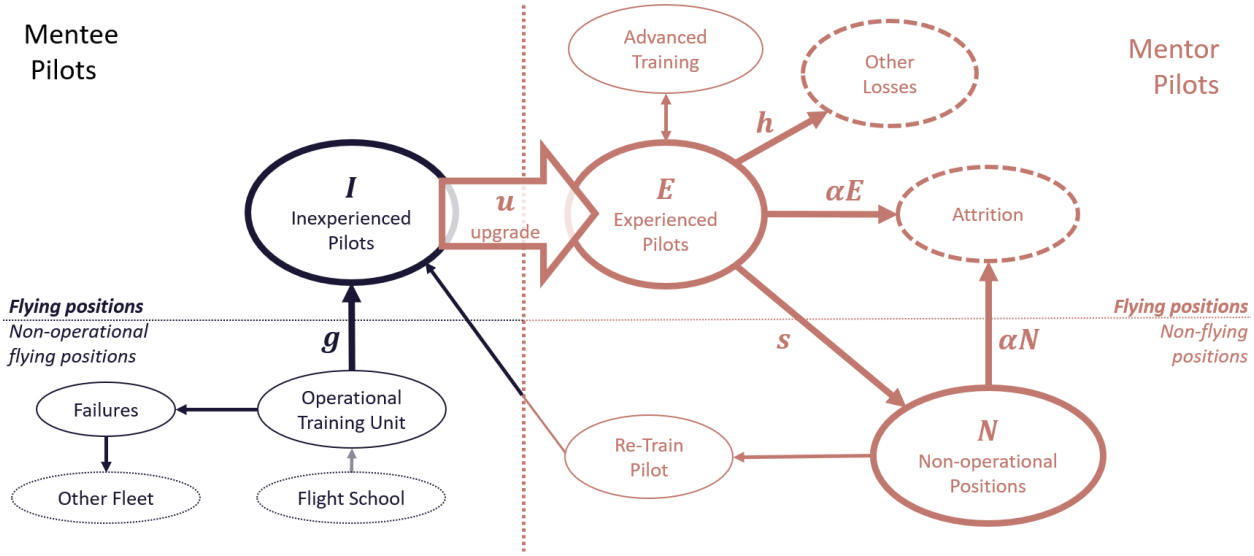

Figure 1: RCAF pilot career flow diagram depicting the principle components of the PARSim model (full) and the MEAD sub-model (bolded).

The parameters of the system must be non-negative, and are as follows:

1. I_0: Initial inexperienced (mentee) population ($t = 0$)
2. E_0: Initial experienced (mentor) population
3. N: Non-operational (staff) population
4. P: Number of authorized flying positions (maximum number of pilots in the operational squadron)
5. R: Number of flying hours required to upgrade
6. g: Operational Training Unit (OTU) graduates (people/year)
7. h: Other losses from the experienced population (people/year)
8. α: Attrition rate parameter (/year)
9. r_I: Maximum inexperienced training rate (hours/year/mentee)
10. r_E: Maximum experienced mentoring rate (hours/year/mentor)
11. r_Y: Maximum overall yearly flying rate (YFR) (hours/year)

MEAD employs some simplifying assumptions to retain mathematical tractability: the minimum number of non-operational positions is always maintained, so staffing flow into N equals attrition flow out to keep N fixed; the return flow from N back to I is ignored, hence s is considered a net flow; there is no attrition from I (an assumption in common with PARSim); h and g are fixed and do not change over time.

From the flow diagram we define a system of differential equations describing the changes in I and E,

$$\frac{dI(t)}{dt} = g - u(t), \tag{1}$$

$$\frac{dE(t)}{dt} = u(t) - (\alpha E(t) + \alpha N + h), \tag{2}$$

$$u(t) = \min \begin{cases} \frac{r_I}{R} I(t) & \text{(mentee-limited)} \\ \frac{r_E}{R} E(t) & \text{(mentor-limited)} \\ \frac{r_Y}{R} & \text{(resource-limited)} \\ \frac{r_E}{R} (P - I(t)) & \text{(position-limited).} \end{cases} \tag{3}$$

The upgrade rate $u(t)$ is the most complex flow in the system and operates in one of four possible domains. At any given time, the upgrade rate may be limited by the maximum rate of training per mentee, r_I, the maximum rate of mentoring per mentor, r_E, the maximum overall flying rate for the fleet, r_Y, or the maximum number of flying positions, P. It is the minimum of these four rates that is the effective rate at a given time. The upgrade rate is always inversely proportional to the number of hours of experience required to upgrade, R, hence this parameter appears in the denominator of the upgrade rate equations. If the total number of pilots, $I + E$, exceeds the number of authorized flying positions, P, then the excess pilots are pushed into non-operational positions, so the effective number of experienced pilots becomes $P - I$. This produces the position-limited upgrade rate, which is a special case of the mentor-limited domain.

3 SYSTEM SOLUTIONS

As described in the preceding section, the system operates in one of four domains depending on which constraint is currently limiting the upgrade rate. Within each domain, the equations can be solved analytically, and this allows us to characterize the behavior of each domain mathematically (Section 3.1), as well as determining the crossover points between domains (Section 3.2) along the system's trajectory. However, there is no analytic solution to the entire model, thus a full solution to MEAD for a given scenario requires numerical simulation, which we illustrate below (Section 3.3).

3.1 The Four Domains

If the system is **mentee-limited** we can solve for $I(t)$ by a change of variables ($X = g - (r_I/R)I$) which allows us to find the solution by separation of variables (exponential) after which we can move back to our original variable (I). For $E(t)$ we can solve via Laplace transformation, where partial fraction decomposition is used to facilitate taking the inverse Laplace transform to get back to the time domain. The solutions are then

$$I(t) = \Delta I e^{-\frac{r_I}{R}t} + I_{SS}, \tag{4}$$

where $\Delta I = I_0 - I_{SS}$ is the difference between the initial inexperienced population level, I_0, and with the steady state level being $I_{SS} = gR/r_I$. And

$$E(t) = \frac{r_I \Delta I}{r_I - \alpha R} \left(e^{-\alpha t} - e^{-\frac{r_I}{R}t} \right) + \Delta E e^{-\alpha t} + E_{SS}, \tag{5}$$

where $\Delta E = E_0 - E_{SS}$ and $E_{SS} = \frac{g-h-\alpha N}{\alpha}$. Note that we have cast the solutions in terms of I_{SS} and E_{SS} as the mentee-limited domain is the only stable domain with finite, positive steady state values.

If the system is **mentor-limited**, we can solve for $I(t)$ and $E(t)$ using the same analytic tools as before and we find

$$I(t) = \frac{-k_1}{1-\frac{\alpha R}{r_E}} e^{\left(\frac{r_E}{R}-\alpha\right)t} + \left(\frac{-h-\alpha N}{1-\frac{\alpha R}{r_E}} + g\right)t + k_2, \text{ and} \tag{6}$$

$$E(t) = k_1 e^{\left(\frac{r_E}{R}-\alpha\right)t} + \frac{h+\alpha N}{\frac{r_E}{R}-\alpha}, \tag{7}$$

$$\text{where } k_1 = E_0 - \frac{h+\alpha N}{\frac{r_E}{R}-\alpha}, \text{ and } k_2 = I_0 - \frac{k_1}{1-\frac{\alpha R}{r_E}}.$$

If the system is **resource-limited**, we can solve for both $I(t)$ and $E(t)$ by change and separation of variables. This yields the solutions:

$$I(t) = I_0 + \left(g - \frac{r_Y}{R}\right)t, \text{ and} \tag{8}$$

$$E(t) = \frac{(E_0\alpha R + k)\, e^{-\alpha t} - k}{\alpha R}, \tag{9}$$

$$\text{where } k = -r_Y + hR + \alpha NR.$$

If the system is **position-limited**, we can solve for $I(t)$ and $E(t)$ obtaining

$$I(t) = k_1 e^{\frac{r_E}{R}t} + P - \frac{gR}{r_E}, \text{ and} \tag{10}$$

$$E(t) = \frac{-k_1}{1+\frac{\alpha R}{r_E}} e^{\frac{r_E}{R}t} + k_2 e^{-\alpha t} + \frac{g-h-\alpha N}{\alpha}, \tag{11}$$

$$\text{where } k_1 = I_0 - P + \frac{gR}{r_E}, \text{ and } k_2 = E_0 + \frac{k_1}{1+\frac{\alpha R}{r_E}} - \frac{g-h-\alpha N}{\alpha}.$$

3.2 Determining Domain Crossover Points

To simulate the population trajectory over time we must determine the points at which crossover between domains will occur. To do so we solve for the intersections of the subfunctions of $u(t)$ depending on the current domain. For example, if the system is initially in the resource-limited domain, we determine the point at which the system will crossover to the mentee-limited domain by solving for t_1 in

$$\frac{r_Y}{R} = \frac{r_I}{R} I(t_1) \Leftrightarrow r_Y = r_I\left(I_0 + \left(g - \frac{r_Y}{R}\right)t_1\right) \Leftrightarrow t_1 = \left(\frac{r_Y}{r_I} - I_0\right) \Big/ \left(g - \frac{r_Y}{R}\right).$$

Similarly, to find when the system will crossover to the mentor-limited domain, we can solve for t_2 in

$$\frac{r_Y}{R} = \frac{r_E}{R} E(t_2) \Leftrightarrow r_Y = r_E\left(\frac{(E_0\alpha R + k)\, e^{-\alpha t_2} - k}{\alpha R}\right) \Leftrightarrow t_2 = \frac{-1}{\alpha} \ln\left(\frac{r_Y \alpha R + r_E k}{r_E\,(E_0\alpha R + k)}\right).$$

To find when the system will crossover to the position-limited domain, we can solve for t_3 in

$$\frac{r_Y}{R} = \frac{r_E}{R}\,(P - I(t_3)) \Leftrightarrow r_Y = r_E\left(P - I_0 - \left(g - \frac{r_Y}{R}\right)t\right) \Leftrightarrow t_3 = \frac{r_E P - r_Y - r_E I_0}{r_E\left(g - \frac{r_Y}{R}\right)}.$$

Finally, the actual crossover point will be at $\min\{t \in (t_1, t_2, t_3) \mid t \in \mathbb{R}_{>0}\}$. If a crossover point t is found, then we can find the next one t' by repeating the process using the new domain and by setting $I_0 = I(t)$ and $E_0 = E(t)$. If no crossover point is found (either no solution exists or the solution is non-positive), then the current domain corresponds to the final domain of the system. Appendix A shows the equations to be solved to find all possible crossover points; ten out of twelve equations for the crossovers are transcendental equations, four of which we must explicitly root find to solve. To find such trajectory crossover points we used SciPy's *optimize.root_scalar* method (Virtanen et al. 2020). We set the objective function to $f(t) = g(t) - h(t)$, where $g(t)$ is the subfunction of $u(t)$ for the current domain and $h(t)$ is the subfunction for the target domain. We use bracketing instead of initial guess to exclude the possibility of the algorithm finding a negative root, as we are interested in future crossovers. We bracket as $[\varepsilon, z]$, where z is a positive real number such that $f(z) > 0$ and ε is a small positive number. Because $g(t)$ is the current upgrade rate, then $g(\varepsilon) < h(\varepsilon) \implies f(\varepsilon) < 0$, satisfying the requirement that we bracket zero (boundary values of different signs). We chose $\varepsilon = 0.000001$ as the bottom limit of the bracket to avoid finding a null crossover point, while maintaining some analytic precision and responsive computation. We find z by iteratively evaluating f at values up to and including 40 years. We chose 40 years as an upper bound as CAF decision makers are not usually interested in results past this threshold and to maintain a reasonably responsive computation time.

For the special case where the initial state of the system falls exactly on a boundary between domains, then the domain it belongs to is considered to be the domain the trajectory will move into.

3.3 Example Scenario

To demonstrate an application of the model we consider a running example with the following parameters: $N = 25$ pilots, $P = 30$ pilots, $R = 250$ hours, $g = 4$ graduates/year, $\alpha = 0.07$ /year, $h = 1$ pilot/year, $r_I = r_E = 144$ hours/year/mentee-mentor, and $r_Y = 1500$ hours/year.

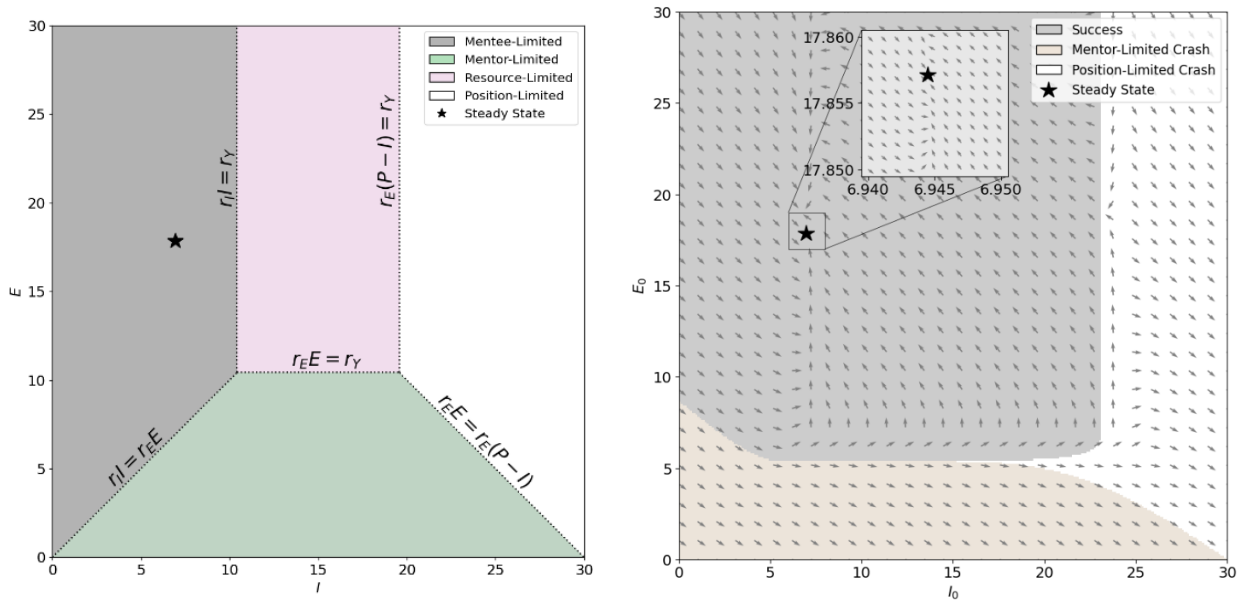

(a) System domains.

(b) Change in system domains.

Figure 2: System phase space.

We first consider the *I*–*E* phase space for our set parameters. The lines marking the separation between the domains in Figure 2a correspond to the equations of the intersections of the subfunctions of $u(t)$

(Section 3.2, Appendix A). Note that if the amount of flying resources are not a limiting factor (i.e., r_Y is large enough), then the pink resource-limited region of the plot would narrow and disappear, and the mentee-limited and position-limited domains would be separated by the line with equation $r_I I = r_E(P-I)$, and the lines $r_I I = r_E E$ and $r_E E = r_E(P-I)$ would intersect to form a triangle delimiting the mentor-limited domain in the bottom part of the plot.

In Figure 2b we can observe how the experienced and inexperienced populations will change over time starting at any given value for I and E, and show the vector field defined by the differential model that indicates the direction of change at each point in the field. The colored areas in the figure define regions of stability: within the grey region, the system is stable and will progress to a steady state condition denoted by the star; within the brown region, the system is unstable and will progress to a mentor-limited collapse, $E = 0$ pilots, along the bottom of the figure; and within the white region, the system is unstable and will progress to a position-limited collapse, $P - I = 0$ pilots, along the right side of the figure. For the system to be stable, several conditions must be met: there must always be a critical minimum number of mentors or the system will progress irreversibly toward a mentor-limited collapse; if the number of mentors is low but not below the critical level, then the number of mentees must be large enough as to not induce a collapse in the mentor-limited domain; and the number of mentees must not exceed a certain critical maximum number or the system will progress irreversibly toward a position-limited collapse. Moreover, historically it was believed that if the number of mentors is low, then the number of mentees should also be kept low in order to stabilize the system. However, this result shows that, in fact, in a low-mentor situation, it is both having too few or too many mentees that can lead to a collapse, assuming no intervention is taken.

The inset plot in Figure 2b shows the behaviour around the steady state (here $I_{SS} \approx 6.944$ pilots and $E_{SS} \approx 17.857$ pilots). We observe that, generally, the system follows a counter-clockwise trajectory to steady state, approaching more aggressively when $I < I_{SS}$ and $E > E_{SS}$ or when $I > I_{SS}$ and $E < E_{SS}$.

By comparing the two graphs in Figure 2, we can observe some common behaviors. For example, in the bottom-left corner of the plots, the system can start in the mentee-limited domain, crossover to the mentor-limited domain and collapse; in the upper right side of the plot, the system can start in the position-limited domain, transition to the resource-limited domain, then to the mentee-limited domain and reach steady state; or, in the bottom right corner of the plots, the system could begin in the mentor-limited domain, crossover to the position-limited domain and collapse.

To analyze specific system paths we consider the population trajectory through the vector field defined by the differential model. On inputting the system parameters plus I_0 and E_0 we can consider the specific trajectory of the system as an overlay to the vector field describing the system, the times at which the system will change domains, collapse, or reach the steady state, and a matching plot showing the variation of $I(t)$ and $E(t)$ through time (see Figure 3). Note that as we asymptotically approach steady state, we define reaching this state as being within 5% of I_{SS} or E_{SS}, a choice motivated by staffing levels of 95% or higher being considered healthy in the CAF (Henderson 2019).

Figure 3 shows example system trajectories near the success versus mentor-limited collapse threshold seen in Figure 2b using the same input parameters. In Figure 3a, the system starts in the mentee-limited domain, crosses to the mentor limited domain after 2.11 years, and collapses after 6.61 years. Therefore, if this system started in January 2025, we can expect the mentor population to be completely depleted by approximately August 2031. Here, we can also observe how sensitive the system can be. For example, having one more mentor will cause the system to deviate towards the steady state (Figure 3b) instead of collapsing (Figure 3a).

4 VERIFICATION

Simulations can most easily be run in practice by solving MEAD's equations numerically. To verify these results, we compared the numerical simulations with the analytical solutions for each domain and crossover points between domains for a number of cases, and we compared MEAD's results to those of PARSim. For the comparison between numerical and analytical solutions, we present a special case where the system

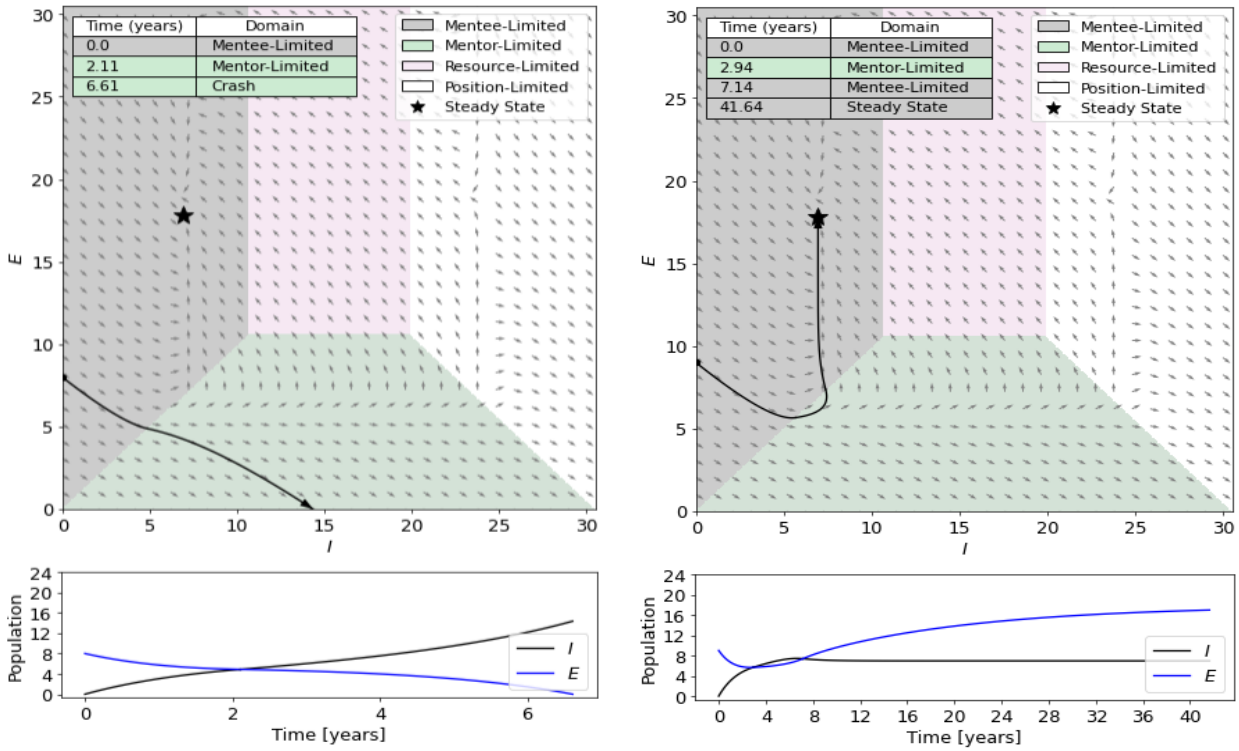

(a) $I_0 = 0$, $E_0 = 8$.

(b) $I_0 = 0$, $E_0 = 9$.

Figure 3: System trajectories for different values of I_0, E_0.

crosses through all four domains, a strong test ($I_0 = 22$ pilots, $E_0 = 7$ pilots). From Equation 1,

$$\frac{\Delta I}{\Delta t} \approx \frac{dI}{dt} = g - u(t), \Delta I = I(t+\Delta t) - I(t) \implies I(t+\Delta t) \approx I(t) + (g - u(t)) \times \Delta t,$$

where Δt is the time step and the differential equation is recovered in the limit. Likewise, from Equation 2,

$$E(t+\Delta t) \approx E(t) + (u(t) - h - \alpha E(t) - \alpha N) \times \Delta t.$$

To determine the trajectory of the system directly from the differential equations we iteratively found $I(t+\Delta t)$ and $E(t+\Delta t)$, calculating $u(t)$ at each timestep and varying the value of Δt for each experiment. Figure 4a compares the analytic trajectory with the one obtained directly from the DE with $\Delta t = 7$ years (the artificially large value selected to allow visual discrimination). Figure 4b shows the mean absolute error (MAE) between both solutions as a function of Δt. As $\Delta t \to 0$ years we see MAE $\to 0$, verifying the analytic solutions and crossovers presented here.

For the verification of MEAD against PARSim, we consider a scenario that is initially far from steady state and observe the initial transient behavior and long term steady state behavior of both models. For PARSim g is specified as entry of one pilot every three months, and for I_0 experience is uniformly distributed on $[0, R]$. Visually the trajectories agree reasonably well (see Figure 4c), and both approach identical steady states to four significant figures ($E_{SS}^{PARSim} = 17.8566$ pilots and $E_{SS}^{MEAD} = 17.8571$ pilots; $I_{SS}^{PARSim} = 6.9443$ pilots and $I_{SS}^{MEAD} = 6.9444$ pilots; where PARSim's steady state was measured over the final 50 years of a 200 year simulation run). The transient differences are an area of ongoing investigation, but can be attributed to PARSim and MEAD implicitly assuming different intake processes and survival distributions for upgrade and attrition (Henderson and Bryce 2019; Bryce and Henderson 2020).

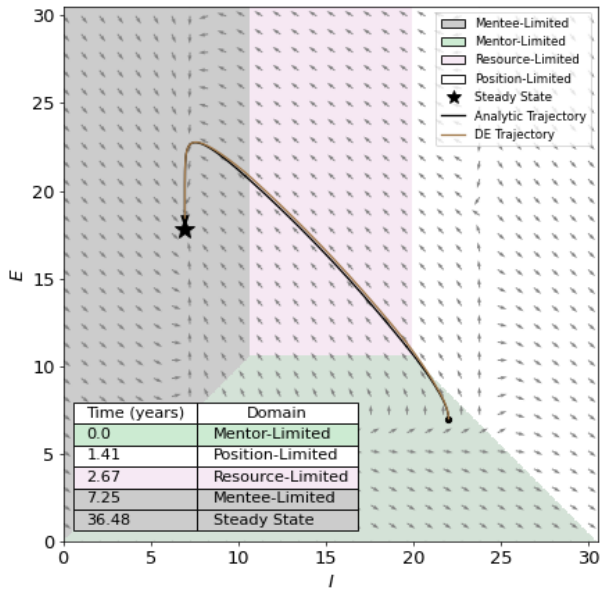

(a) Comparison of the trajectories with Δt = 7 years.

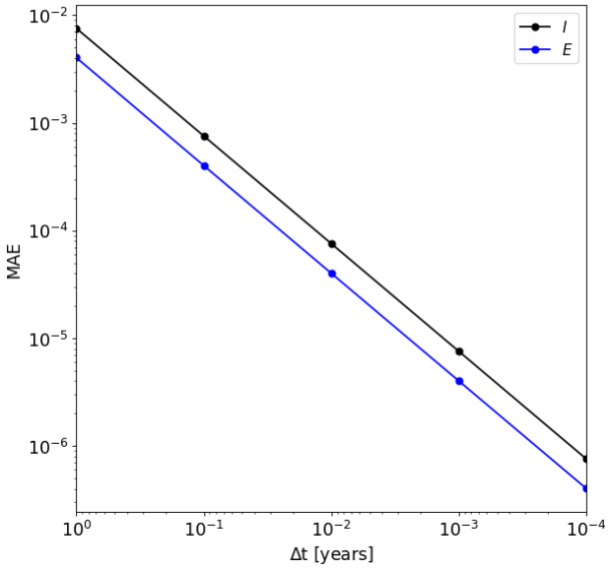

(b) The MAE with varying values of Δt.

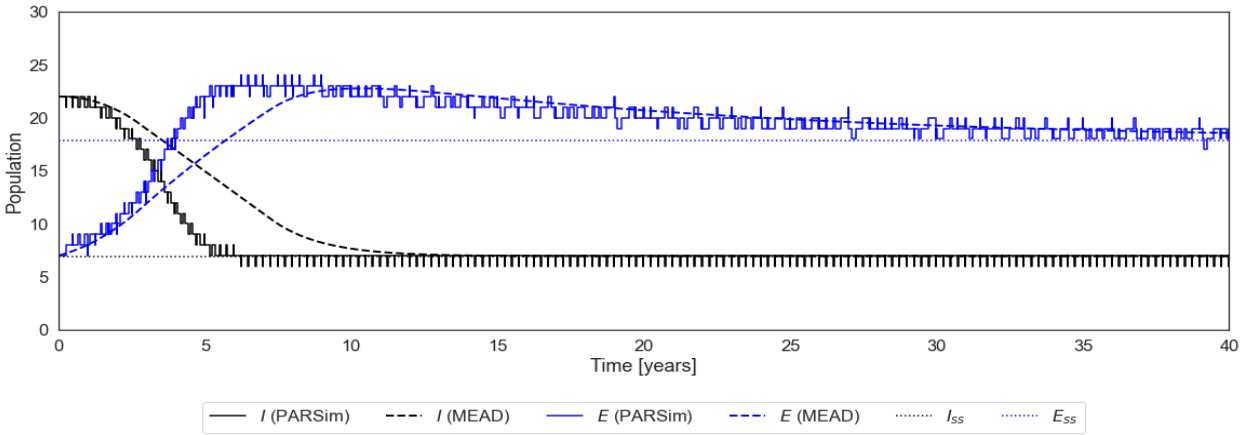

(c) PARSim versus MEAD trajectories.

Figure 4: Verification of analytic solutions.

5 DISCUSSION

Inspecting the vector fields of a given MEAD parameterization, one can observe certain critical values. In Figure 3 in the mentor-limited (green) region, there is a critical value for the mentor population, E_{crit}, above which the vector field progresses upwards toward a possible stable solution, and below which the vector field progresses downwards toward a collapse. Likewise, for the position-limited (white) region there is a critical value for the mentee population, I_{crit}, below which the vector field progresses to the left toward a possible stable solution, and above which the vector field progresses to the right toward a collapse. These critical values can be determined by inspecting the underlying differential model (Equations 1 and 2, and upgrade model 3). For the **mentor-limited** region we find $E_{crit} = (h + \alpha N)/(\frac{r_E}{R} - \alpha)$, as determined by setting dE/dt (Equation 2) to zero, which equals approximately 5.4 pilots for our example. It is of note that this critical value is highly sensitive to α. Similarly, for the **position-limited** region $I_{crit} = P - \frac{gR}{r_E}$, giving approximately 23.1 pilots for our example. Above this value I will increase and the effective number of

experienced pilots, $P-I$, will be driven to zero. Below this value the system will either be driven to steady state or approach a resource limited special case. For the **resource-limited** region if $dI/dt = 0$ we have a special case where for intake g equal to the resource limit $r_Y/R = 6.25$ /year for our parameterization, then $I(t) = I_0$ for all t and $E(t) \to E_{SS}$, however this is a metastable solution and any small deviation will push the system out of equilibrium in I. If $g > r_Y/R$, the system will progress into the position limited region, if $g < r_Y/R$, the system will progress into the mentee-limited region. We observe that the **mentee-limited** domain is the only domain in which the system is stable and approaches a steady state condition, and that if E ever drops below E_{crit} (critically mentor-limited), or if I ever exceeds I_{crit} (critically position-limited), the system will irreversibly collapse.

The mentor population will have an increased effective attrition rate parameter over α, due to the requirement to maintain the non-operational positions N (see Figure 1). As the attrition rate parameter fixes the number of people flowing out, by definition, we have $out = \alpha \int_t^{t+1} E dt \approx \alpha E$ (see (Bryce and Henderson 2023)), and rearranging we have $\alpha = out/E$. As the number flowing out of E is both due to true loss (attrition) and movement to N to replace the attrition from N, we have $out = \alpha E + \alpha N + h$ (see Equation 2) and so the effective attrition rate is $\alpha_{eff} = \alpha(1 + N/E) + h/E$ and we get an "enhanced", or increased, attrition rate that is inflated. As a sufficient number of mentors is required to absorb mentees into a squadron both α and N are important control parameters when attempting to confront situations where the mentor population level is too low. We note that in steady state, the flow into E must equal g, and the inflow to E must equal the outflow. From $out \approx \alpha E$ and the steady state constraints we find $E_{SS} = g/\alpha_{eff} \approx 17.857$ pilots for the parameters used in our running example, agreeing with MEAD.

Here we made simplifications to the full model of pilot flow as captured in PARSim. The goal was two-fold, one was to allow a simple to implement and responsive tool that could be used at the staff level and by decision makers, and the second was to facilitate finding parameters that are plausibly achievable and appear to lead to a healthy state over time—and then explore these more extensively in PARSim. We are currently modelling two aircraft fleet transitions, the fighter transition from the CF-18 Hornet to the F-35 Lightning, and the Canadian Multi-Mission Aircraft (CMMA) transition from the CP-140 Aurora to the P-8A Poseidon, and will be exploring where a MEAD versus PARSim approach is advantageous and carefully contrasting the models.

By modifying various parameters where partial control mechanisms may exist such as attrition (α, h), the number of OTU graduates (g), staff positions (N), and other parameters, the sensitivity and stability of the system can be explored and appropriate planning and risk mitigation measures can take place. To facilitate changing parameters and exploring what-if scenarios, we created a web tool where parameters can be set by sliders and input boxes, and a number of plots are generated (including the figures reported here, in addition to several others). The intent is to enable both analysts, who traditionally have performed such what-if exploration, as well as staff and decision makers, to explore and understand the response of the system to various parameterizations.

We presented preliminary results to the RCAF Fighter Capability Office (FCO) to obtain feedback regarding the potential usefulness of the web tool for staff and decision makers. They saw value in the interactivity and ability to quickly answer what-if questions. In particular, being able to discern the upgrade limiting domains through which the population trajectory passes (e.g., Figure 4a) and how long it would take to approach steady state were seen as beneficial. Future work will include carefully assessing differences between PARSim and MEAD and working with military staff and senior officers to deploy and support the tool for RCAF usage.

6 CONCLUSION

We have developed a judiciously simplified differential equation model, MEAD, of a detailed DES pilot occupation model, PARSim. MEAD reproduces the key dynamics and inter-relationships present in PARSim while being orders of magnitude faster to setup and execute for conducting simulations. Due to its simplified implementation and very fast execution speed, a web tool was developed that accepts user

inputs for parameters and initial conditions describing a pilot occupation, and returns a number of graphs communicating how the initial populations will evolve over time as well as regions in the parameter phase space that are healthy (stable and leading to a non-zero steady state) and unhealthy (unstable and leading to population collapse). Our analytical analysis of MEAD's system of equations leads to the discovery of steady state conditions and certain critical values that bound the regions of stability and instability. These insights were not possible without MEAD's mathematical description of the pilot career structure. An advantage of the web tool is it enables staff and decision makers to run what-if scenarios themselves, allowing intuition to be built and specific scenarios to be investigated. One key feature of the pilot structure is its sensitivity to the mentor population size, and small changes in parameters can lead to large changes in outcome. This makes a sensitivity analysis and understanding of how unstable the system can be in some regions of the parameter phase space important, and MEAD and the associated web tool facilitate such analysis and build such understanding.

ACKNOWLEDGMENTS

We would like to thank Lieutenant Colonel Reid McBride, Major Brian Bews, and Dr. Slawo Wesolkowski of the Royal Canadian Air Force for their feedback and guidance.

A UPGRADE DOMAIN CROSSOVER EQUATIONS

Here we collect all the domain crossover equations, see Section 3.2 for discussion.

Table 1: Crossover equations for all possible domain changes.

Initial Domain	Target Domain	Crossover Equation
Mentee-Limited	Mentor-Limited	$r_I\left(\Delta I e^{-\frac{r_I}{R}t}+I_{SS}\right)=r_E\left(\frac{r_I\Delta I}{r_I-\alpha R}\left(e^{-\alpha t}-e^{-\frac{r_I}{R}t}\right)+\Delta E e^{-\alpha t}+E_{SS}\right)$
	Resource-Limited	$t=\frac{-R}{r_I}\ln\left(\left(\frac{r_Y}{r_I}-I_{SS}\right)/\Delta I\right)$
	Position-Limited	$t=\frac{-R}{r_I}\ln\left(\frac{r_E P-r_E I_{SS}-r_I I_{SS}}{\Delta I(r_I+r_E)}\right)$
Mentor-Limited	Mentee-Limited	$r_E\left(k_1 e^{\left(\frac{r_E}{R}-\alpha\right)t}+\frac{h+\alpha N}{\frac{r_E}{R}-\alpha}\right)=r_I\left(\frac{-k_1}{1-\frac{\alpha R}{r_E}}e^{\left(\frac{r_E}{R}-\alpha\right)t}+\left(\frac{-h-\alpha N}{1-\frac{\alpha R}{r_E}}+g\right)t+k_2\right)$
	Resource-Limited	$t=\frac{1}{\frac{r_E}{R}-\alpha}\ln\left(\frac{r_Y}{r_E k_1}-\frac{h+\alpha N}{k_1\left(\frac{r_E}{R}-\alpha\right)}\right)$
	Position-Limited	$P-\left(\frac{-k_1}{1-\frac{\alpha R}{r_E}}e^{\left(\frac{r_E}{R}-\alpha\right)t}+\left(\frac{-h-\alpha N}{1-\frac{\alpha R}{r_E}}+g\right)t+k_2\right)=k_1 e^{\left(\frac{r_E}{R}-\alpha\right)t}+\frac{h+\alpha N}{\frac{r_E}{R}-\alpha}$
Resource-Limited	Mentee-Limited	$t=\left(\frac{r_Y}{r_I}-I_0\right)\Big/\left(g-\frac{r_Y}{R}\right)$
	Mentor-Limited	$t=\frac{-1}{\alpha}\ln\left(\frac{r_Y\alpha R+r_E k}{r_E(E_0\alpha R+k)}\right)$
	Position-Limited	$t=\frac{r_E P-r_Y-r_E I_0}{r_E\left(g-\frac{r_Y}{R}\right)}$
Position-Limited	Mentee-Limited	$t=\frac{R}{r_E}\ln\left(\frac{gR\left(1+\frac{r_I}{r_E}\right)-r_I P}{k_1(r_I+r_E)}\right)$
	Mentor-Limited	$-k_1 e^{\frac{r_E}{R}t}+\frac{gR}{r_E}=\frac{-k_1}{1+\frac{\alpha R}{r_E}}e^{\frac{r_E}{R}t}+k_2 e^{-\alpha t}+\frac{g-h-\alpha N}{\alpha}$
	Resource-Limited	$t=\frac{R}{r_E}\ln\left(\frac{gR-r_Y}{r_E k_1}\right)$

REFERENCES

Bartholomew, D., A. Forbes, and S. McClean. 1991. *Statistical Techniques for Manpower Planning*. 2nd ed. Chichester, West Sussex: John Wiley & Sons.

Boileau, M. 2012. "Workforce Modelling Tools Used by the Canadian Forces". In *Proceedings of The International Workshop on Applied Modelling & Simulation*. September 24th-27th, Cosenza, Italy, 18-23.

Bryce, R. M. and J. A. Henderson. 2020. "Workforce Populations: Empirical Versus Markovian Dynamics". In *2020 Winter Simulation Conference (WSC)*, 1983–1993 https://doi.org/10.1109/WSC48552.2020.9384030.

Bryce, R. M. and J. A. Henderson. 2023. "Estimating Workforce Attrition Rate Parameters: A Controlled Comparison". In *Proceedings of the 12th International Conference on Operations Research and Enterprise Systems*, edited by F. Liberatore, S. Wesolkowski, and G. H. Parlier, 82–93. Setúbal: Science and Technology Publications, Lda.

Corbett, N. C. 2013. "Modelling the Production and Absorption of Pilots: The Development of the Production Absorption and Retention Simulation (PARSim)". Technical Report DRDC CORA TR 2013-023, Defence Research and Development Canada, Ottawa, Canada. https://cradpdf.drdc-rddc.gc.ca/PDFS/unc121/p537222_A1b.pdf, accessed 20th August 2024.

Henderson, J. A. 2019. "The Force Flow Model: A Discrete Event Simulation for Military Personnel Planning". Technical Report DRDC-RDDC-2019-R214, Defence Research and Development Canada, Ottawa, Canada. https://cradpdf.drdc-rddc.gc.ca/PDFS/unc342/p811387_A1b.pdf, accessed 20th August 2024.

Henderson, J. A. and R. M. Bryce. 2019. "Verification Methodology for Discrete Event Simulation Models of Personnel in the Canadian Armed Forces". In *2019 Winter Simulation Conference (WSC)*, 2479–2490 https://doi.org/10.1109/WSC40007.2019.9004841.

Lahteenmaa-Swerdlyk, T. and F.-A. Bourque. 2024. "Investigation of Workforce Dynamical Behaviour from a Phase Plane Perspective". In *Proceedings of the 13th International Conference on Operations Research and Enterprise Systems*, edited by F. Liberatore, S. Wesolkowski, and G. H. Parlier, 35–46. Setúbal: Science and Technology Publications, Lda.

Mattock, M. G., B. J. Asch, J. Hosek, and M. Boito. 2019. "The Relative Cost-Effectiveness of Retaining Versus Accessing Air Force Pilots". Technical Report RR-2415-AF, RAND Corporation. https://www.rand.org/pubs/research_reports/RR2415.html, accessed 20th August 2024.

Okazawa, S. 2013. "A Discrete Event Simulation Environment Tailored to the Needs of Military Human Resources Management". In *2013 Winter Simulation Conference (WSC)*, 2784–2795 https://doi.org/10.1109/WSC.2013.6721649.

ORIGAME GitHub repository. 2024. https://github.com/DND-DRDC-RDDC/OS_ORIGAME, accessed 14th March.

Schaffel, S., F.-A. Bourque, and S. Wesolkowski. 2021. "Modelling the Mentee-Mentor Population Dynamics: Continuous and Discrete Approaches". In *2021 Winter Simulation Conference (WSC)*, 1–10 https://doi.org/10.1109/WSC52266.2021.9715289.

Seal, H. 1945. "The Mathematics of a Population Composed of K Strata Each Recruited from the Stratum Below and Supported at the Lowest Level by a Uniform Annual Number of Entrants". *Biometrica* 33(3):226–230.

Séguin, R. 2015. "PARSim, a Simulation Model of the Royal Canadian Air Force (RCAF) Pilot Occupation". In *Proceedings of the 4th International Conference on Operations Research and Enterprise Systems*, edited by B. Vitoriano and G. H. Parlier, 51–62. Setúbal: Science and Technology Publications, Lda.

Vincent, E. and S. Okazawa. 2019. "Determining Equilibrium Staffing Flows in the Canadian Department of National Defence Public Servant Workforce". In *Proceedings of the 8th International Conference on Operations Research and Enterprise Systems*, edited by G. H. Parlier, F. Liberatore, and M. Demange, 205–212. Setúbal: Science and Technology Publications, Lda.

Virtanen, P., R. Gommers, T. E. Oliphant, M. Haberland, T. Reddy, D. Cournapeau *et al*. 2020. "SciPy 1.0: Fundamental Algorithms for Scientific Computing in Python". *Nature Methods* 17(3):261–272.

AUTHOR BIOGRAPHIES

JACK QUIRION is an undergraduate student in Computer Science and Mathematics at the University of Ottawa and a CO-OP student at the Defence Research and Development Canada (DRDC) Centre for Operational Research and Analysis (CORA). He plans on pursuing graduate studies in discrete mathematics and theoretical computer science. Contact via email at jquir073@uottawa.ca.

STEPHEN OKAZAWA is a Defence Scientist with the Centre for Operational Research and Analysis in Defence Research and Development Canada in Ottawa, Canada. He holds a masters degree in Electro-Mechanical Engineering from the University of British Columbia, Canada. His research focuses on modelling and simulation of military personnel systems, especially using discrete event simulation methods. Contact via email at stephen.okazawa@forces.gc.ca.

ROBERT MARK BRYCE is a Defence Scientist at the Department of National Defence. Holding a PhD in Physics from the University of Alberta, Robert Mark's research interests lie in explanatory data analysis—using theory, modeling, simulations, machine learning, graphing, and other tools. Contact via email at Robert.Bryce@forces.gc.ca.

JILLIAN ANNE HENDERSON is a Defence Scientist at the Defence Research and Development Canada (DRDC) Centre for Operational Research and Analysis (CORA). Dr. Henderson holds a doctorate in Science (Astronomy) from the Universidad Nacional Autónoma de México (UNAM). Her research interests lie in numerical modelling and simulation with a current focus on strategic military personnel management. Contact via email at jillian.henderson@forces.gc.ca.